

Proposal of double-sided type transverse flux linear synchronous motor

Shin Jung-Seob and Takafumi Koseki

The University of Tokyo, Engineering Building #2 12F,7-3-1 Hongo, Bunkyo-ku, Tokyo 113-8656, Japan
jungseobshin1008@koseki.t.u-tokyo.ac.jp, koseki@koseki.t.u-tokyo.ac.jp

Kim Hounng-Joong

Sung-Jin Royal Motion Co. Ltd, 103-1311, Digital Empire 2, Sin-dong 486, Yeongtong-gu, Suwon, Gyeonggi-do, 443-734, Korea

kimh3000@naver.com

ABSTRACT: Linear motors have been a great interest from industries. Especially, linear synchronous motor that uses rare earth permanent magnets in the field side (PMLSM) has contributed to the popularization in industrial fields because of its high efficiency and compact size. However, the thrust force density could not be largely enhanced in conventional PMLSM due to the space competitions between the stator teeth and armature conductors. In recent years, the transverse flux PM-type linear synchronous motor has been researched as alternative because it can inherently offer high thrust density. We propose a double-sided transverse flux PMLSM. In this paper, the concept and structure of the proposed model are introduced and its characteristics are both theoretically analyzed and numerically computed by field calculation using Finite Element Method (FEM).

1 INTRODUCTION

Linear motors are being employed increasingly in industrial fields. Such direct devices offer many advantages over ball-skew drive, which result in a higher dynamic performance and reliability.

There are many types of linear motors including linear synchronous motor, linear induction motor and linear stepping motor etc. Especially, linear synchronous motor that uses permanent magnets (PMLSM) in the field side has contributed to the popularization in industrial fields because of the advent of rare earth permanent magnet, which results in high efficiency and compact size.

However, conventional longitudinal flux type PMLSM whose drawback is low thrust density has a limitation in their applications. How to obtain high thrust density is one of the most significant investigation subject today.

Referring to high thrust density machines, the transverse flux machine is an ideal alternative [1].

However, conventional transverse flux machine has such complex manufacturing requirements that it is impractical for industrial production.

In this paper, we propose a double-sided transverse flux PMLSM. Also, the fundamental concept and structure of the proposed model are introduced and its characteristics are both theoretically analyzed and numerically computed by field calculation using FEM.

2 PROPOSAL OF DOUBLE-SIDED TRANSVERSE FLUX PMLSM

The armature side consists of I-type core, coil in order to generate travelling field. One armature core has basically four salient poles and armature coils are wound around each salient pole as shown in Fig. 1 (a).

In the field side, one field unit consists of four magnets, back yoke and non-material spacer as

shown in Fig. 1 (b). By one armature unit and field unit, one magnetic circuit has achieved in the proposed model as shown in Fig. 1 (c).

Also, the armature and field side of the proposed model can be simply fabricated by laminated steel, which is a large improvement compared with conventional transverse flux machine.

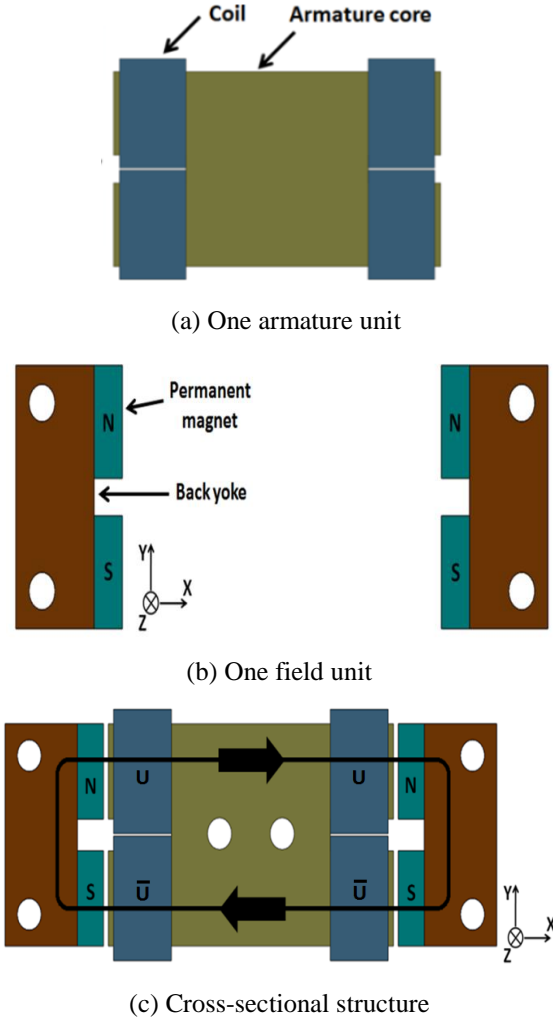


Figure 1. Structure of the proposed model.

In the case of moving direction, three armature cores are arranged to moving direction Z with non-magnetic material spacer as shown in Fig. 2.

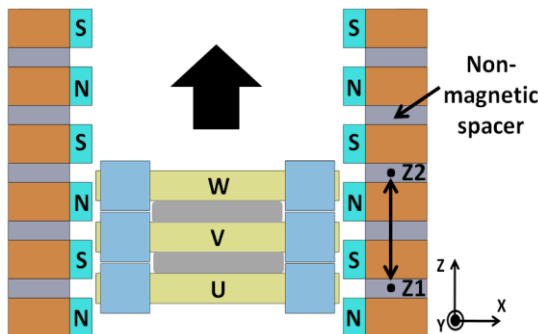


Figure 2. Fundamental configuration of three-phase units of the proposed model.

Each armature core is apart with 120 degrees spatially. By adding AC current which has 120 degree phase difference to each armature core, the proposed motor drives as 3-phase AC synchronous machinery. Also, non-magnetic material spacer between cores in the armature and field side can achieve magnetic separation of each core. The distance between point Z1 and point Z2 in Fig. 2 is one mechanical period in the moving direction.

3 PROPOSAL CHARACTERISTICS OF I-TYPE ARMATURE CORE COMPARED WITH CONVENTIONAL C-TYPE CORE

General conventional transverse flux type PMLSM has C-type armature core. In the proposed model, I-type armature core is employed [2].

However, I-type armature core in the proposed model has some characteristics compared with general C-type core.

First, Winding is relatively easy because it is enough to insert coil in each salient pole. In C-type core, armature core had been to segmented two parts in order to save space for winding. For that reason, simplification of component and easy production will be achieved in I-type core.

Second, magnetic saturation of armature core can be problem in C-type core because winding is concentrated in one core back. However, in the proposed model, magnetic saturation of armature core can be relatively low because of four separated winding in one armature core, which is connected to low core loss, high performance, high thrust-current characteristics and efficiency.

In order to confirm magnetic saturation, we compared I-type core with general C-type core and applied three-dimensional analysis to one magnetic circuit of the proposed model and C-type PMLSM as shown in Fig. 3. One of the results is shown in Fig. 4.

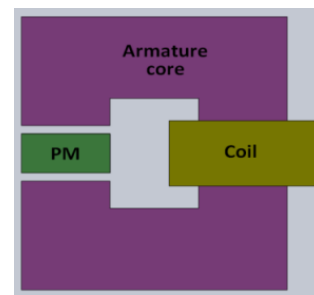


Figure 3. General C-type core of transverse flux PMLSM.

In the same condition of magnetic circuit included in a same dimension of flux path, air gap, 240 winding turns and magnets, air gap flux density and

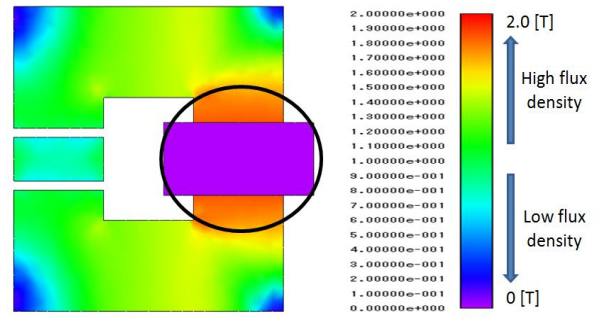
flux density in core wound coil of the proposed model is 0.92T and 1.24T respectively. In this time, current added to coil is 5A and each salient pole has 60 turns.

However, in C-type core configuration made in order to obtain a same air gap flux density, flux density in core wound coil is 1.93T and it exceeds the operating point considered linear region of the armature core (50JN230, JFE Steel Corp.)[3]. This is because of a concentrated magnetomotive force (MMF) in one place. In the result shown in Fig. 4 (b) and (c), it is also clear that an effect of magnetic saturation of core is higher in C-type, which can be connected to high core loss, low performance, low thrust-current characteristics and efficiency.

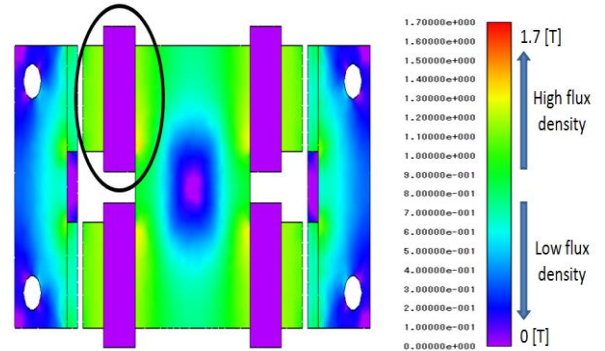
Moreover, from three-dimensional FEM results of current-flux density characteristics in the air gap and core as shown in Fig. 5, it is found that the air gap flux density in C-type is saturated by increasing current added to the armature coil because of the effect of magnetic saturation.

If dimension of flux path wound coil increases in order to prevent magnetic saturation of core in C-type, coil end, total volume, the amount of material and copper loss also increase at a time, which can cause deterioration of efficiency.

Third, it is possible to decrease saturation of thrust by increasing armature current. From static thrust-armature current characteristics as shown in Fig. 6, theoretical value is nearly same with three-dimensional FEM value to 10A. Static thrust starts to saturate because of magnetic saturation of core. However, static thrust in C-type core model is saturated in 5A. Also it is relatively lower than that in the proposed model. This is because of magnetic saturation of armature core in C-type core where winding is concentrated in one core back and small area thrust can generate. In the proposed model, thrust can be generated in four areas but only two areas in C-type model.

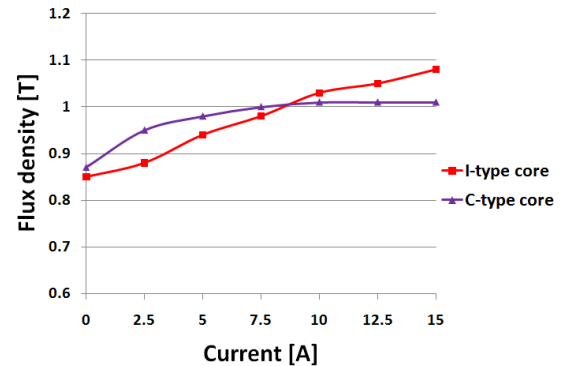


(b) The flux density distribution of C-type PMLSM

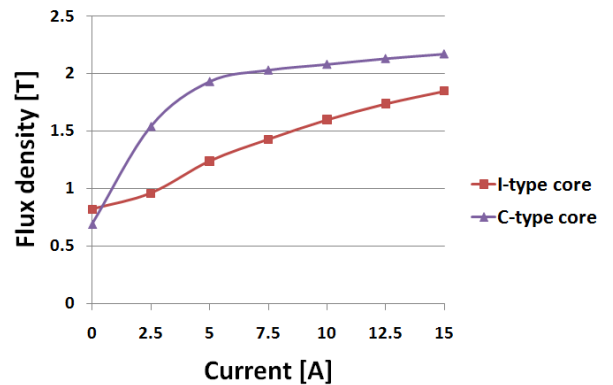


(c) The flux density distribution of the proposed model

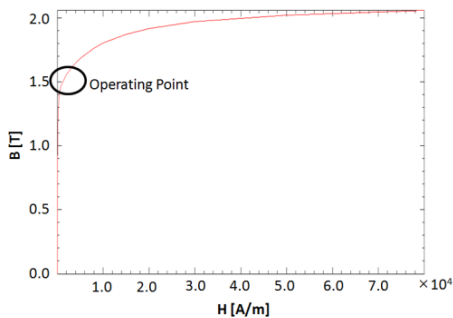
Figure 4. The result of three-dimensional FEM analysis.



(a) The air gap flux density



(b) B-H curve of 50JN230 (JFE Steel Corp.)



(a) B-H curve of 50JN230 (JFE Steel Corp.)

Figure 5. The current-flux density characteristics.

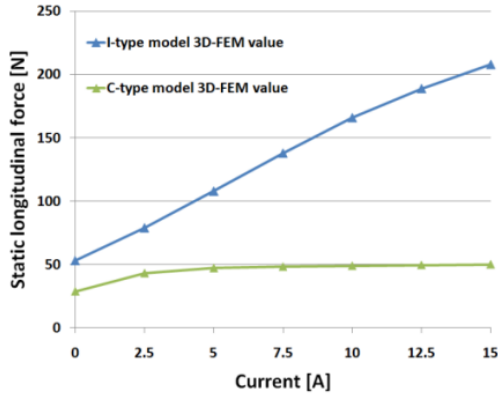


Figure 6. Static thrust-armature current characteristics of the proposed model and C-type based model.

4 ESTIMATION OF FUNDAMENTAL CHARACTERISTICS BY THEORETICAL METHOD

We have employed magnetic circuit method in order to estimate characteristics of the proposed model theoretically.

In the proposed model, a armature core consists of one magnetic circuits as shown in Fig. 1(c) when the armature side is above the field side. In order to estimate characteristics of the proposed model simply, we have considered one magnetic circuit as shown in Fig. 7. Also, they assumed the permeability of armature and field cores are infinitely large.

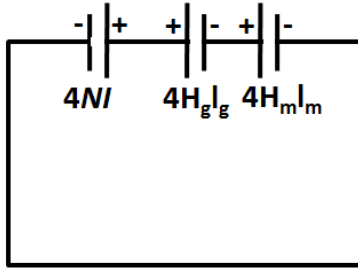


Figure 7. Equivalent configuration and magnetic circuit considering one magnetic circuit.

From Fig. 7, one magnetic circuit can be expressed as

$$NI = H_g l_g + H_m l_m \quad [A] \quad (1)$$

where H_m , H_g are the magnetic-field component of magnet and the air gap, l_g , l_m is the length of the air gap and magnet, I is armature current and N is the turn number of a winding of an armature pole.

If the permeability of armature and field cores is infinite, the magnet flux density B_m in operating point can be expressed as (2). B_r is remanence of magnet and μ_0 is permeability of the air gap.

$$B_m = B_r + \mu_0 H_m \quad [T] \quad (2)$$

Also, the air gap flux density B_g , the air gap flux ϕ_g and the magnet flux ϕ_m can be calculated as follows. In equation (4) and (5), A_m , A_g are the dimension of magnet and air gap.

$$B_g = \mu_0 H_g \quad [T] \quad (3)$$

$$\phi_g = B_g \times A_g \quad [Wb] \quad (4)$$

$$\phi_m = B_m \times A_m \quad [Wb] \quad (5)$$

By using equations from (1) to (5), The air gap flux density B_g can be written as (6).

$$B_g = \frac{k_l B_r}{\frac{A_g}{A_m} + \frac{g_d}{l_m}} \left(1 - \frac{NI}{H_c l_m} \right) [T] \quad (6)$$

In equation (6), H_c is the coercive force of magnet, k_l is flux leakage coefficient, g_d is the air gap length considered cater coefficient.

If the air gap flux distribution of one armature pole can be modeled as shown in Fig. 8 by moving one armature core, the air gap flux and its density can be expressed by Fourier series. Its fundamental component is (7).

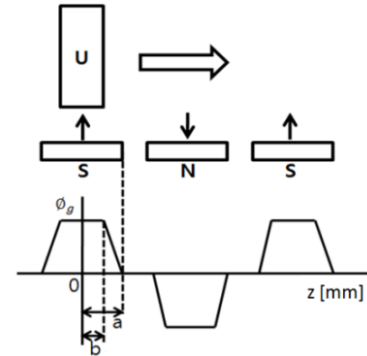


Figure 8. The air gap flux distribution by moving one armature core.

$$\begin{aligned} \phi_g(z) &= \frac{4\phi_{g\tau}}{(b-a)\pi^2} \left\{ \cos\left(\frac{\pi a}{\tau}\right) - \cos\left(\frac{\pi b}{\tau}\right) \right\} \cos\left(\frac{\pi z}{\tau}\right) \\ &= \phi_{gmax} \cos\left(\frac{\pi z}{\tau}\right) \quad [Wb] \end{aligned}$$

$$B_g(z) = \phi_g(z) A_g = B_{gmax} \cos\left(\frac{\pi z}{\tau}\right) \quad [T] \quad (7)$$

In equation (7), ϕ_{gmax} , B_{gmax} are the maximum value of the air gap flux and its density, τ is pole pitch, a and b are the half length of one field magnet and one armature core respectively.

Hence, the back electromotive force (EMF) and its root mean square (RMS) value can be obtained as (8). In equation (8), p is the number of pole in one field unit, v is the moving velocity, k_c is winding factor and z is the distance to moving direction.

$$e(z) = -k_c p N \frac{d\phi_g}{dt} = \frac{k_c k_l \pi v p N \phi_{gmax}}{\tau} \sin\left(\frac{\pi z}{\tau}\right) [V]$$

$$E_{rms} = \frac{0.707 k_c k_l \pi v p N \phi_{gmax}}{\tau} [V] \quad (8)$$

The total thrust and maximum thrust density based on the dimension and the volume in nine slot-eight pole combination can be derived as (9), (10) and (11). “Dimension” means dimension of the space in which the armature side is faced with the field side. “Total volume” means volume of the space in which total armature and field side occupy.

$$F_{thrust}(z) = \sum \frac{0.707 k_c k_l \pi v p N I \phi_{gmax}}{\tau} \sin\left(\frac{\pi z}{\tau} + 2(\theta - 1)\right), (\theta: 1 \sim 9) [N]$$

$$F_{thrust_max} = 1.5 \times \frac{0.707 k_c k_l \pi v p N I \phi_{gmax}}{\tau} [N] \quad (9)$$

$$F_{dimension} = \frac{F_{thrust_max}}{\text{Dimension}} [N/m^2] \quad (10)$$

$$F_{volume} = \frac{F_{thrust_max}}{\text{Total volume}} [N/m^3] \quad (11)$$

From virtual work principle, detent force per an armature core in the proposed model can be derived as (12).

$$F_{detent}(z) = -\frac{dW}{dz} = -\frac{d}{dz} \left(\frac{B_g^2(z) V_g}{2\mu_0} \right)$$

$$= \frac{k_l^2 B_{gmax}^2 \pi A_g g d}{2\mu_0 \tau} \sin\left(\frac{2\pi z}{\tau}\right) [N]$$

$$F_{detent_max} = \frac{k_l^2 B_{gmax}^2 \pi A_g g d}{2\mu_0 \tau} [N] \quad (12)$$

In (12), V_g is the air gap volume. It is found that the period of detent force is the same with pole pitch τ electrically. The main characteristics based on theoretical values in the proposed model are shown in Table I.

5 NUMERICAL PERFORMANCE EVALUATION OF THE PROPOSED MODEL USING FEM

We applied three-dimensional FEM field analysis to the proposed model for rational verification of fundamental characteristics.

5.1 Detent force

The reduction of detent force in PMLSM is one of the most important factors required in industrial fields and this can affect to high positioning accuracy. Many methods to reduce detent force in PMLSM have been reported included in skewing, semi-closed slots and magnet length optimization etc [4]. However, these methods can be a burden in the

manufacturing stage and sometimes affect to manufacturing cost.

We focused on slot-pole combination to reduce detent force. In the case of rotational synchronous machinery, the higher Least Common Multiple (LCM) of slot-pole is, the lower cogging torque can be achieved.

Since drive principle of linear synchronous machine is the same with rotational synchronous machine, we applied nine slot-eight pole combination to the proposed model in the stage of selecting numbers of armature cores and field poles [5]. Hence, nine armature cores are faced with eight magnets in one electric period as shown in Fig. 9.

$$F_{detent_total}(z) = \sum \frac{k_l^2 B_{gmax}^2 \pi A_g g d}{2\mu_0 \tau} \sin\left(\frac{2\pi z}{\tau} + 2(\theta - 1)\right), (\theta: 1 \sim 9) [N] \quad (13)$$

$$I_{second} = \frac{180 \times S}{\tau} \times \frac{\text{the number of slot}}{\text{the number of pole}}$$

$$I_{third} = \frac{180 \times 2S}{\tau} \times \frac{\text{the number of slot}}{\text{the number of pole}} \quad (14)$$

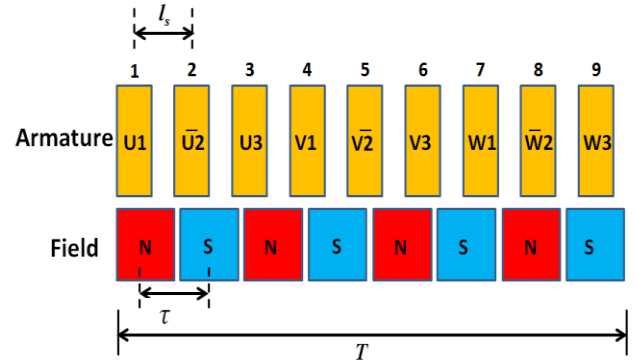


Figure 9. Configuration of nine armature cores and eight field magnets.

If a pole pitch is 9mm and U-phase current is applied to the first core, the total distance T is 72mm and the distance S between the first and the second cores is 8mm. Hence, the second and the third cores has 160 and 320 degrees phase difference from the first core, respectively. It means that detent force of each core has electrically 20 degrees phase shift. Consequently, the total detent force can be calculated as in equation (13) when considering fundamental component of detent force. In equation (13), θ is the number of each core in Fig. 9. From equation (14), the current applied to the second and the third windings have 180 and 360 degree phase difference from the first winding. Also, if the total distance T is 360 degrees electrically, each armature core has 40 degree phase difference electrically. Hence, the fourth and the seventh cores have 120 and 240 degree

phase difference from the first core. Also, the fifth and the eighth cores have 120 and 240 degree phase difference from the second core. In this principle, the current added to the armature coil is changed from U-V-W in three slot-two pole combination as shown in Fig. 2 to $U - \bar{U} - U - V - \bar{V} - V - W - \bar{W} - W$ ($\bar{U}, \bar{V}, \bar{W}$ are the current components shifted 180 degrees from U,V,W.).

The result of detent force in three-dimensional FEM analysis is shown in Fig. 10. The maximum value of detent force could be reduced to about 2.3N when three armature cores moved in one mechanical period which is the distance from point Z1 to point Z2 as shown in Fig. 2 and its wave form was nearly sinusoidal. Hence, high positioning accuracy could be achieved in the proposed model.

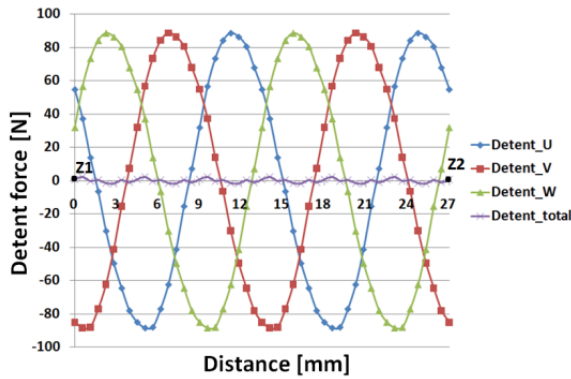


Figure 10. Detent force of the proposed model.

5.2 Thrust

This results of the proposed model considered three cores per one phase in $I = 5A$, $N = 67$ turns is shown in Fig. 11.

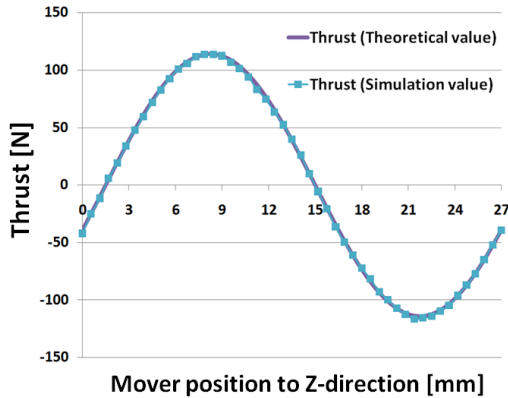


Figure 11. Thrust of the proposed model.

As shown in Fig. 11, the maximum value of thrust was 139.98N in three-dimensional FEM analysis of the proposed model and it was the nearly same with theoretical value which is 114.06. When considering three phase model, the maximum value of thrust is 171N.

5.3 Normal attractive force by magnetic unbalance

In principle, the normal attractive force can be cancelled in double-sided PMLSM. In this condition, the air gap length at both side is the same and magnetic balance is maintained.

However, if the field side is not supported robustly or the air gap length at both side is not the same by machining error, magnetic balance in the air gap is disrupted. This disruption of magnetic balance leads to the normal attractive force between the armature side and the field side, which can cause thrust ripple, noise and performance deterioration, etc.

The normal attractive force can be expressed as (15).

$$F_x = F_{x_{left}} - F_{x_{right}} \\ = \frac{S}{\mu_0} (B_{gmax_left}^2 - B_{gmax_right}^2) \text{ [N]} \quad (15)$$

In equation (15), $F_{x_{left}}, F_{x_{right}}$ are normal attractive force acted in the left and right side, $B_{gmax_left}, B_{gmax_right}$ are the maximum air gap flux density in the left and right side, S is dimension of the air gap.

From equation (15), it is found that normal attractive force is not generated when magnetic balance is maintained in the air gap.

In order to deliberate the normal attractive force, we applied three-dimensional FEM analysis to the proposed model. In three-dimensional FEM analysis, we considered the model in which the armature side is moved 0.5mm to the right side. One of the result is shown in Fig. 12.

Normal attractive force was changed by moving armature core and its average value was 36.4N. The maximum normal attractive force was 51.6N and caused when the armature core is above the field magnet. However, it was not generated when magnetic balance is maintained in the air gap.

This means it is important that the field side has to be supported robustly in order to withstand 51.6N at least and careful assembly and fabrication are needed.

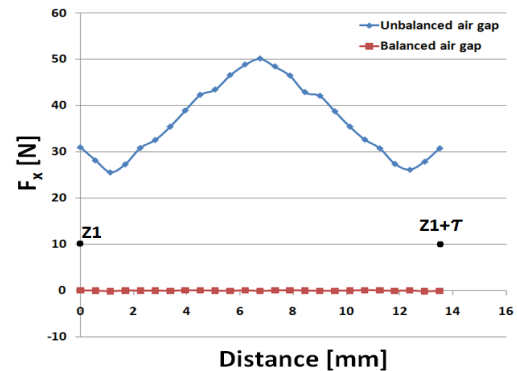


Figure 12. Normal attractive force by moving armature core.

6 CONCLUSION

In this paper, a double-sided transverse flux PMLSM is proposed.

The armature and field side of the proposed model can be simply fabricated by laminated steel, which is a large structural improvement compared with conventional transverse flux machine.

Compared with general C-type armature core in transverse flux type machinery, I-type core in the proposed model has advantages included in easy winding works and low magnetic saturation by separated winding, which could result in high dynamic performance.

Also, its characteristics are theoretically calculated and numerically analyzed by FEM. Especially, the details of the theoretical characteristics allowed for understanding of the fundamental behavior of the proposed model without complex calculation.

In FEM analysis, detent force was reduced to about 2.3N by nine slot-eight pole combination. This is 1.35% of total thrust. Hence, a high positioning accuracy could be achieved in the proposed model.

In principle, the normal attractive force can be cancelled. However, it is important that the field side has to be supported robustly and careful assembly and fabrication are needed.

Future work will involve further characterization of the prototype through static and dynamic testing including thrust density, thrust ripple and positioning accuracy.

Also, evaluation through comparison with commercial PMLSM's will be conducted in order to validate effectiveness of the proposed model.

Table I Theoretical characteristics of the proposed model

1 armature size [mm]	1 field size [mm]	1 magnet size [mm]
57w×35h×7d	15w×9d	5.4w×15h×9d
Turn number of a winding of an armature pole N [turns]	1 non-magnetic spacer size [mm]	Air gap length g_a [mm]
67	15w×4.5d	1.27
Slot-pole combination	Pole pitch τ [mm]	Slot pitch [mm]
9-8	13.5	12
Flux leakage coefficient k_l	Back EMF E_{rms} in one armature unit [V]	Armature current I [A]
0.99	7.92	5
Moving velocity v [m/s]	Maximum thrust $F_{thrust,max}$ in one armature core [N]	Maximum detent force $F_{detent,max}$ in one armature core [N]
1	39.62	35.34
**Maximum thrust density F_{volume} [N/m ³]	**Maximum thrust density $F_{dimension}$ [N/m ²]	The number of magnet in one field unit
39.6×10^4	2.02×10^4	4

* is based on three-dimensional FEM analysis

** is based on in nine slot-eight pole combination

7 REFERENCE

- Weh. H, Hoffman. H, Landrath. J : "New Permanent Magnet Excited Synchronous Machine with High Efficiency at Low Speeds", Proceedings of the International Conference on Electrical Machines, 1988.
- K. Sato, J. S. Shin, T. Koseki and Y. Aoyama : "Basic Experiments for High-Torque, Low-Speed Permanent Magnet Synchronous Motor and a Technique for Reducing Cogging Torque", International Conference on Electrical Machines, ICEM 2010.
- JFE Steel Corp.
www.jfe-steel.co.jp/
- Z. Guo, L. Chang, Y. Xue : "Cogging torque of permanent magnet electric machines: an overview," Canadian Conference Electrical and Computer Engineering, CCECE '09, pp. 1172-1177, 2009.
- T. Kenjo, S. Nagamori : "Brushless motors : advanced theory and modern applications", Sogo Electronics Press, 2000.